Published OnlineFirst July 28, 2009; DOI: 10.1158/0008-5472.CAN-09-0994

Suppressor of Cytokine Signaling 3 Sensitizes Anaplastic Thyroid Cancer to Standard Chemotherapy

Maria Giovanna Francipane,[1] Vincenzo Eterno,[1] Valentina Spina,[1] Miriam Bini,[1] Gregorio Scerrino,[2] Giuseppe Buscemi,[2] Gaspare Gulotta,[2] Matilde Todaro,[1] Francesco Dieli,[3] Ruggero De Maria,[4,5] and Giorgio Stassi[1]

Departments of [1]Surgical and Oncological Sciences, [2]GENURTO, and [3]Biopathology and Biomedical Methodologies, University of Palermo, Palermo, Italy; [4]Department of Hematology and Oncology, Istituto Superiore di Sanità, Rome, Italy; and [5]Mediterranean Institute of Oncology, Catania, Italy

Abstract

We previously showed that cancer cells from papillary, follicular, and anaplastic thyroid carcinomas produce interleukin-4 and interleukin-10, which counteract the cytotoxic activity of conventional chemotherapy through the up-regulation of antiapoptotic molecules. Here, we identify Janus kinase/signal transducers and activators of transcription (STAT) and phosphatidyl inositol 3-kinase (PI3K)/AKT as the down-stream pathways through which these cytokines confer resistance to cell death in thyroid cancer. We found that the absence of suppressors of cytokine signaling (SOCS) molecules allows the propagation of the survival signaling. Exogenous expression of SOCS1, SOCS3, and SOCS5 in the highly aggressive anaplastic thyroid cancer cells reduces or abolishes STAT3 and 6 phosphorylation and PI3K/Akt pathway activation resulting in alteration in the balance of proapoptotic and antiapoptotic molecules and sensitization to chemotherapeutic drugs *in vitro*. Likewise, exogenous expression of SOCS3 significantly reduces tumor growth and potently enhances the efficacy of chemotherapy *in vivo*. Our results indicate that SOCS3 regulation of cytokines-prosurvival programs might represent a new strategy to overcome the resistance to chemotherapy-induced cell death of thyroid cancer. [Cancer Res 2009;69(15):6141–8]

Introduction

Thyroid carcinomas are the most common endocrine tumors in humans, with a globally increasing incidence. Differentiated tumors, such as papillary (PTC) and follicular (FTC) thyroid cancers, are often curable with surgical resection and radiotherapy (1), whereas undifferentiated (anaplastic) thyroid carcinoma (UTC) is invariably lethal, due to the high invasiveness and insensitivity to radioiodine or chemotherapeutic treatment. We previously reported that autocrine production of interleukin (IL)-4 and IL-10 promotes thyroid cancer resistance to death ligand– and chemotherapy-induced cell death (2, 3). Subsequently, we showed that IL-4 and to a lesser extent IL-10, are also responsible for the growth and resistance to cell death of cancer cells from colon, breast, and lung primary tumors (4, 5).

Requests for reprints: Giorgio Stassi, University of Palermo, Via Liborio Giuffre', 5, Palermo, 90127, Italy. Phone: 011-0039-091-6553211; Fax: 011-0039-091-6553238; E-mail: gstassi@tiscali.it and Ruggero De Maria, Istituto Superiore di Sanità, Viale Regina Elena, 299, Rome, 00161, Italy. Phone: 011-0039-06-49903393; Fax: 011-0039-06-49387087; E-mail: demaria@iss.it.

doi:10.1158/0008-5472.CAN-09-0994

IL-4 signaling propagates through two related pathways. One is initiated with recruitment to IL-4 receptor α (IL-4Rα) of signal transducer and activator of transcription (STAT) 6, following activation of Janus kinase (JAK) 1; the other involves recruitment to the IL-4Rα of insulin receptor substrate-2 (IRS-2, and to a lesser extent IRS-1) with consequential recruitment of phosphatidyl inositol 3-kinase (PI3K), generation of phosphoinositides, and activation of downstream kinases (i.e., Akt) critically involved in cell proliferation and resistance to apoptosis (6). IL-10 receptor (IL-10R) activates JAK1, which in turn initiates phosphorylation of the IL-10Rα leading to STAT3 activation (7). Moreover, there is evidence to suggest that JAK1 phosphorylates IRS-1 docking molecule following interaction with IL-10 with its corresponding receptor. Therefore, activation of PI3K/Akt pathway can occur also following IL-10R triggering (8).

Activated STATs dimerize and migrate to the nucleus, where they activate the transcription of specific genes among which are members of the suppressors of cytokine signaling (SOCS) family (9). SOCS family consists of eight members sharing a central Src-homology 2 domain and a 40 residue COOH-terminal motif called the SOCS box. The Src-homology 2 domain allows different SOCS proteins to bind to specific phosphotyrosines and inhibit cytokine signaling in a classic negative feedback loop, which involves the interaction with cytokine receptors and/or receptor-associated JAKs with consequent inhibition of kinase activity (10). SOCS box is believed to be involved in the degradation of proteins through the ubiquitin-dependent proteosomal pathway (10). Among SOCS molecules, SOCS1, SOCS3, and SOCS5 are mainly involved in the regulation of IL-4 and IL-10 pathways. Both SOCS1 and SOCS3 inhibit JAK tyrosine kinase activity through the kinase inhibitory region at their NH_2 terminus (11). SOCS1 directly binds to the activation loop of JAKs through the Src-homology 2 domain, whereas SOCS3 can inhibit the action of JAK only in the presence of a receptor to which it is believed to bind (11). Studies with SOCS1- or SOCS3-deficient mice indicate that SOCS1 is primarily a negative regulator of IFN-γ signaling (12), whereas SOCS3 is primarily a negative regulator of IL-6 signaling (11). However, both SOCS1 and SOCS3 can be activated by IL-4 or IL-10 and function as potent inhibitors of IL-4/STAT6 or IL-10/STAT3 activation (13). Although SOCS5 function is less clear, it is believed to inhibit IL-4 signaling by binding to the IL-4Rα chain and preventing the interaction with JAK1 (14).

Herein, we found that resistance to chemotherapy in thyroid cancer directly correlates with down-regulation of SOCS molecules. Exogenous expression of SOCS family members in UTC results in growth arrest of a considerable percentage of cells and sensitization of the residual tumor population to cytotoxic drugs.

Published OnlineFirst July 28, 2009; DOI: 10.1158/0008-5472.CAN-09-0994

Materials and Methods

Specimens. Thyroid tissues were obtained from surgical removal from patients affected by PTC (n = 10; age, 47 ± 4 y), FTC (n = 10; age, 55 ± 3 y), and UTC (n = 5; age, 68 ± 7 y), in accordance with the ethical standards of the Institutional Responsible Committee on human experimentation. Control thyroid specimens were obtained from the uninvolved lobes of tumor-affected glands (n = 10; age, 58 ± 10 y). Tumor diagnosis was assessed on the bases of the peculiar histologic features.

Cell purification and culture. Purification of normal and cancer thyroid cells was performed as previously described (2). Fresh epithelial thyroid cells were purified from the digested tumor specimens by hematopoietic cell depletion with anti-CD45 double magnetic bead passage (MACS; Miltenyi Biotec) and red cells lysis. UTC-adherent cell population was obtained after three culture passages of CD45-depleted thyroid tumor cells in the presence of DMEM (EuroClone Ltd.) with 10% heat-inactivated fetal bovine serum (Hyclone Laboratories). Peripheral blood mononuclear cells (PBMC) from healthy volunteers were isolated from heparinized blood by Ficoll-Hypaque gradient centrifugation. For cytokine stimulation, normal thyrocytes, anaplastic thyroid cancer cells, and PBMCs were exposed to human recombinant IL-4 (20 ng/mL) and IL-10 (40 ng/mL) for 24 h in RPMI 1640 (Euroclone).

Protein isolation and immunoblotting. Cell pellets were resuspended in ice-cold NP40 lysis buffer [50 mmol/L Tris-HCl (pH 7.5), 150 mmol/L NaCl, 1 mmol/L EGTA, and 1% NP40] containing proteases and phosphatases inhibitors as previously described (2). Lysates were fractioned on SDS-polyacrylamide gels and blotted to nitrocellulose. Membranes were blocked for 1 h with nonfat dry milk in TBS containing 0.05% Tween 20 and successively incubated with antibodies specific for phospho-Jak1 [3331, Tyr1022/1023, rabbit polyclonal; Cell Signaling Technology (CST)], Jak1 (3332, rabbit polyclonal; CST), phospho-STAT6 (9361, Tyr641, rabbit polyclonal; CST), STAT6 (9362, rabbit polyclonal; CST), phospho-STAT3 (9131, Tyr705, rabbit polyclonal; CST), STAT3 (9132, rabbit polyclonal; CST), phospho-Akt (9271, Ser 473, rabbit polyclonal; CST), Akt (9272, rabbit polyclonal; CST), phospho-GSK3β (9336, Ser9, rabbit polyclonal; CST), GSK3β (9315, rabbit polyclonal; CST), Cyclin D1 (DCS6, mouse IgG2$_a$; CST), p27^{Kip1} (2552, rabbit polyclonal; CST), phospho-IKKα (2681, Ser180)/IKKβ (Ser181, rabbit polyclonal, CST), phospho IκB-α (9241, Ser32, rabbit polyclonal; CST), Bak, (06-536, NT, rabbit polyclonal; Upstate Biotechnology), Mcl-1 (S-19, sc-819, rabbit IgG; Santa Cruz Biotecnology), Bax (06-499, NT, rabbit polyclonal; Upstate Biotechnology), Noxa (N-15, SC-26917, goat polyclonal; Santa Cruz Biotecnology), Bcl-xL (H-5, mouse IgG1; Santa Cruz Biotechnology, Inc.), Bcl-2 (05-729, clone 100, mouse IgG1; Upstate Biotechnology), pBad (9295, Ser136, rabbit polyclonal; CST), HA (clone 16B12, mouse IgG1; Babco), and β-actin (Ab-1 mouse IgM; Calbiochem). Membranes were then washed, incubated for 1 h with horseradish peroxidase–conjugated anti-mouse, anti-rabbit, or anti-goat immunoglobulins (Amersham Biosciences UK Limited), and developed with a chemiluminescence detection system (SuperSignal West Pico/Dura Extended duration Substrate; Pierce Biotechnology).

Immunohistochemistry, immunofluorescence, H&E, Azan Mallory, and *in situ* TUNEL. Stainings were performed on 6-μm-thick paraffin-embedded sections of human thyroid tissues and of tumor xenografts, on thyroid cell monolayers and on cytospun thyroid cancer cells. Sections or monolayers were incubated with 1% human serum from AB donors for 20 min to block unspecific staining, followed by incubation with specific antibodies against phospho-Akt (4051, Ser 473, 587F11 mouse IgG2b; CST), phospho-GSK3β (9336, Ser9, rabbit polyclonal; CST), nuclear factor-κB (NF-κB; 3032, rabbit polyclonal; CST), phospho-STAT6 (9361, Tyr641, rabbit polyclonal; CST), phospho-STAT3 (9131, Tyr705, rabbit polyclonal; CST), or isotype-matched controls for 1 h at room temperature. Then, sections or monolayers were washed in TBS, incubated with biotinylated anti-mouse or anti-rabbit immunoglobulins for 30 min, and treated with streptavidin-peroxidase (LSAB 2 kit; Dako Corporation). Stainings were revealed using 3-amino-9-ethylcarbazole (red color) substrate and counterstained with aqueous hematoxylin (blue color). For immunofluorescence, cytospun thyroid cancer cells were fixed with 2% paraformaldehyde for 20 min at 37°C, washed in PBS, and exposed for 1 h at 37°C to antibodies against IL-4 (BMS129, Clone B-S4, mouse IgG1; Bender System, Inc.), IL-10 (BMS131/2, Clone B-T10, mouse IgG1; Bender System), IL-4Rα (sc-684, c-20, rabbit IgG; Santa Cruz Biotecnology), IL-10R (sc-984, c-20, rabbit IgG; Santa Cruz Biotecnology), phospho-STAT6 (9361, Tyr641, rabbit polyclonal; CST), phospho-STAT3 (9131, Tyr705, rabbit polyclonal; CST), NF-κB p65 (RelA; AB1604, rabbit IgG; Chemicon International), GSK3β (9315, rabbit polyclonal; CST), or phospho-GSK3β (9336, Ser9, rabbit polyclonal, CST). Then, cells were treated with FITC- or Rhodamine Red–conjugated anti-mouse or anti-rabbit antibodies (Molecular Probes, Inc.) plus RNasi (200 ng/mL) and counterstained using Toto-3 iodide (642/660; Molecular Probes). Confocal analysis was used to acquire fluorescence stainings.

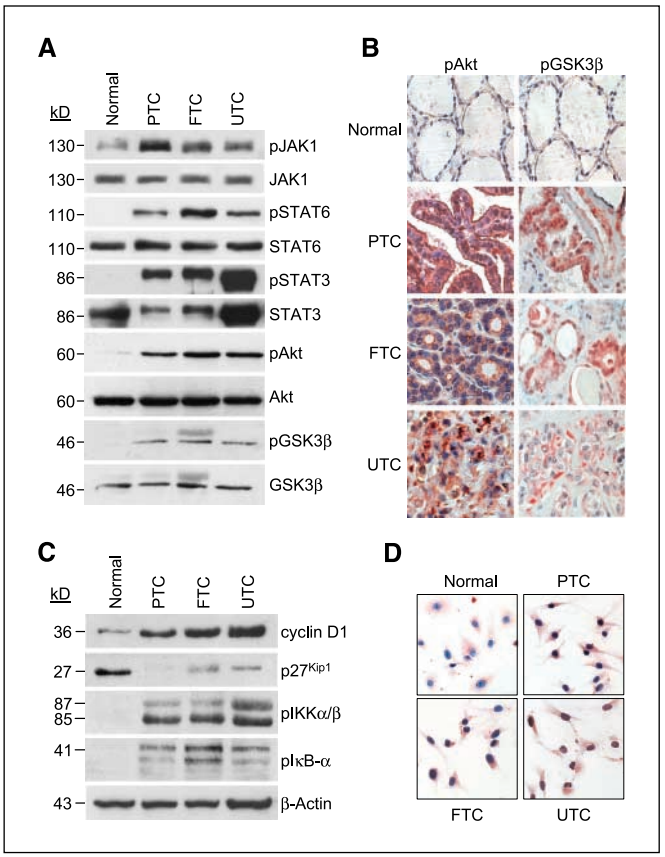

Figure 1. JAK/STAT and PI3K/Akt pathways are activated in thyroid cancer cells. *A,* Western blot analysis of pJAK1, pSTAT6, pSTAT3, pAkt, and pGSK3β in freshly purified normal thyroid, PTC, FTC, and UTC cells. Loading control was performed by using JAK1, STAT6, STAT3, Akt, and GSK3β respectively, in the same membrane. *B,* immunohistochemical analysis (*red staining*) of pAkt and pGSK3β in normal thyroid, PTC, FTC, and UTC paraffin-embedded sections. *C,* immunoblot analysis of cyclin D1, p27^{Kip1}, pIKKα/β, and pIκB-α, performed on normal and PTC, FTC, and UTC thyrocytes. Loading control was performed by using β-actin. *D,* immunocytochemical analysis of NF-κB on thyroid normal and cancer monolayer cells. One representative of five immunoblots and one of three immunohisto/cytochemical analyses are shown.

For H&E staining, dewaxed sections were stained in hematoxylin for 5 min, washed in water, and then exposed for 1 min to eosin. For Azan Mallory (A.M.), sections were stained with azocarmine G (nuclei, red color) for 1 h and with 5% of phosphovolframic acid for an additional hour. Then, sections were stained with aniline blue/orange G and mounted in synthetic resin. Apoptosis was determined by *In Situ* Cell Death Detection, AP kit (Boehringer Mannheim). DNA strand breaks were detected by 5-bromo-4-chloro-3-indolyl-phosphate (BCIP; Dako; dark blue color) substrate.

Real-time PCR. Total RNA from cell pellets was obtained using the Rneasy Mini kit (Qiagen GmbH) and retrotranscribed using High-Capacity

Published OnlineFirst July 28, 2009; DOI: 10.1158/0008-5472.CAN-09-0994

cDNA Archive kit (Applied Biosystems) according to manufacturer's instructions. Quantitative Taqman PCR analysis was performed with the ABI PRISM 7900HT Sequence Detection System (Applied Biosystem) in a reaction volume of 25 μL containing 1× TaqmanUniversal Master Mix (Applied Biosystems) and 1× probes and primer sets Hs00705164_s1 (SOCS1; Taqman Gene Expression Assays, Applied Biosystems), Hs00269575_s1 (SOCS3; Taqman Gene Expression Assays, Applied Biosystems), Hs00751962_s1 (SOCS5; Taqman Gene Expression Assays, Applied Biosystems), or 1× Hu glyceraldehyde-3-phosphate dehydrogenase (GAPDH; Pre-Developed Taqman Assay Reagents; Applied Biosystems). The thermal profile was follows: 95°C for 10 min and 35 cycles at 95°C for 15 s and 60°C for 1 min. All amplification reactions were done in triplicate, and the relative quantitation of SOCS genes expression was calculated using the comparative Ct method (ΔΔCt). Levels of mRNA expression were expressed after normalization with endogenous control, GAPDH. Data processing and statistical analysis were performed using the ABI PRISM SDS, software version 2.1 (Applied Biosystems).

Production of lentiviral particles and infection. Full-length cDNA clones for SOCS1 (IRAKp961J1182Q), SOCS3 (IRAKp961B21133Q), and SOCS5 (DKFZp434C198Q) were purchased from ImaGenes GmbH requiring EST sequences verification. HA-tagged Akt_{K179M} was kindly provided by Prof. G.L. Condorelli (Laboratory of Genetic and Molecular Cardiology, Scientific and Technology Pole, IRCCS MultiMedica, Milan, Italy). Gene transfer was performed using TWEEN lentiviral vector containing the green fluorescent protein (GFP) as reporter gene. SOCS1, 3, 5, and Akt_{K179M} cDNAs were subcloned in EcoRV site of the vector. Lentiviral supernatants were collected following 48-h transfection of the packaging human embryonic kidney cell line HEK-293T using calcium phosphate. Then, 10^5 dissociated UTC cells were exposed to 1 mL of viral supernatant of empty vector, SOCS1, SOCS3, SOCS5, or Akt_{K179M}, for 40 min by centrifugating at 800 rpm, in the presence of 8 μg/mL polybrene to improve infection efficiency. After three cycles of infection, cells were washed and cultured in fresh medium. Infection efficiency was evaluated after 72 h by monitoring GFP expression, by reverse transcription-PCR (RT-PCR), or by immunoblot analyses.

Reverse-transcription PCR. Oligonucleotide primers for RT-PCR were designed according to the published sequences (*Genbank Accession numbers*: SOCS1, NM_003745.1; SOCS3, NM_003955.3; SOCS5, NM_194449.2; GAPDH, NM_002046). The primers used were as follows: SOCS1 forward primer, 5′-TTC CGC ACA TTC CGT TCG-3′; SOCS1 reverse primer, 5′-CTG CCA TCC AGG TGA AAG-3′; SOCS3 forward primer, 5′-TCA CCC ACA GCA AGT TTC-3′; SOCS3 reverse primer, 5′-GGA GTA GAT ATA GGC TC-3′; SOCS5 forward primer, 5′-TCT AGA AAT CCC GCC CCT CTA AAG-3′; SOCS5 reverse primer, 5′-CTC GAG GAA AAA GCC TAA CAC TGC TAC G-3′; GAPDH forward primer (870-889), 5′-TGA CAT CAA GAA GGT GGT GA-3′; GAPDH reverse primer (1060-1079), 5′-TCC ACC ACC CTG TTG CTG TA-3′. RT-PCR was performed using the following conditions: SOCS1: 95°C for 1 min, 53°C for 45 s, 72°C for 1 min, 30 cycles; SOCS3: 95°C for 1 min, 52°C for 45 s, 72°C for 45 s, 30 cycles; SOCS5: 95°C for 1 min and 30 s, 59°C for 45 s, 72°C for 1 min and 30 s, 30 cycles; GAPDH: 95°C for 30 s, 53°C for 30 s, 72°C for 1 min, 30 cycles.

Cell viability. Cell viability was evaluated in UTC cells transduced with empty vector, SOCS1, SOCS3, or SOCS5 and treated with Taxol (5 μmol/L; Sigma) or Doxorubicin (5 μmol/L; Sigma), for 24, 48, or 72 h. The number of viable cells was detected using CellTiter Aqueous Assay kit (Promega Corporation) accordingly to manufacturer's instructions. HuT78 cells plated at 2×10^5/mL and treated with an agonistic anti-CD95 antibody (CH-11; 200 ng/mL) were used as a positive control for cell death measurement. Death of empty vector, SOCS1, SOCS3, or SOCS5 after treatment with chemotherapeutic agents was also analyzed by ethidium bromide staining.

Transfections. Normal thyrocytes were cultured in six-well plates for 12 h before transfection with antisense RNA oligonucleotides directed to SOCS1 (5′-CTACCTGAGCTCCTTCCCCTTTTTT-3′) or SOCS3 (5′-AAGACC-CAGTCTGGGACCAAGAATTTTTT-3′) or with a scrambled control oligonucleotide (5′-Fluoro-GAAGTTGAATTCAAGTCGACTTTTTT-3′) by using FuGENE 6 Reagent (Roche). Transfection efficiency was verified by monitoring fluorescent signal from cells transfected with the scramble oligonucleotide and by RT-PCR for SOCS1 or SOCS3.

Animals and tumor model. Five- to 6-wk-old female athymic (nu+/nu+) mice, obtained from Charles River Laboratories, were used. Mice were maintained according to institutional guidelines of animal care and

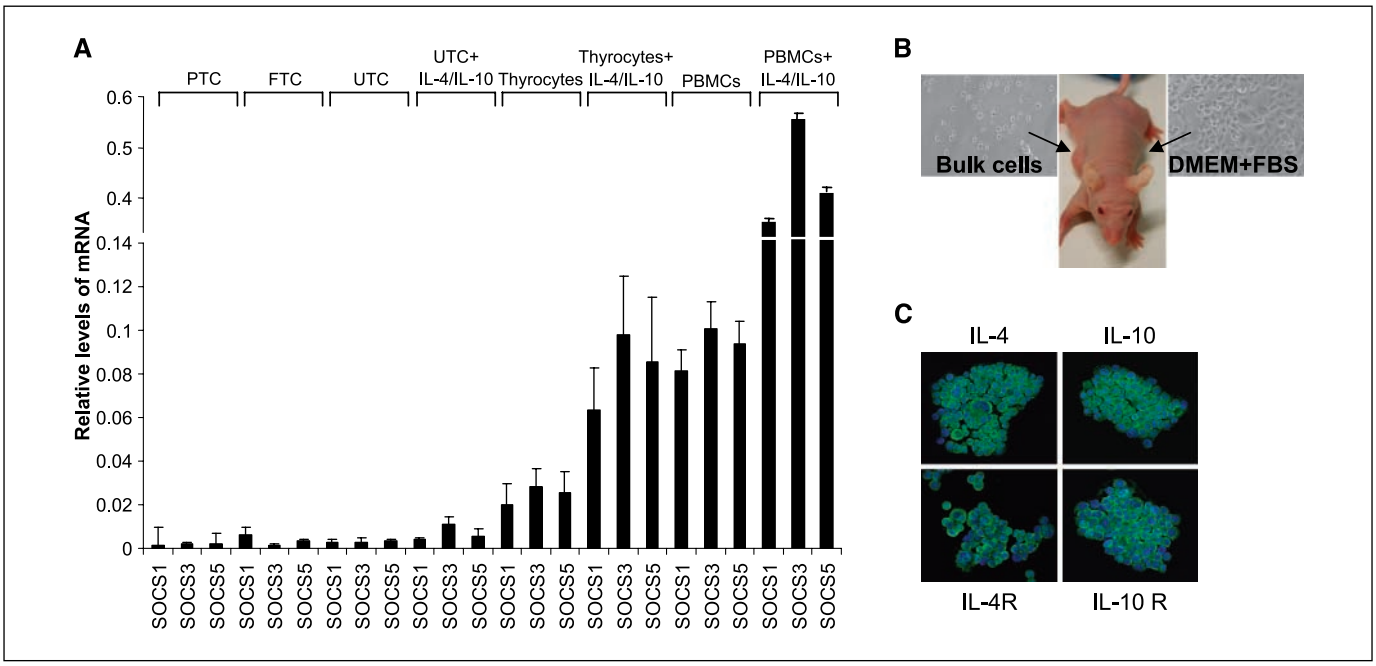

Figure 2. Thyroid cancer cells express low levels of SOCS molecules and express IL-4, IL-10, and their respective receptors. *A,* real-time PCR analysis for SOCS1, 3, and 5 in PTC, FTC, and untreated or IL-4 (20 ng/mL)/IL-10–treated (40 ng/mL) UTC, normal thyrocytes, and PBMCs. *B,* representative picture of injection of both freshly isolated and thrice-passed thyroid cancer cells in nude mice. *C,* immunofluorescence analysis of IL-4, IL-10, IL-4Rα and IL-10R in UTC cytospun cells (*green*). Nuclei were stained with Toto-3 iodide (*blue*). One representative of three independent experiments is shown.

Published OnlineFirst July 28, 2009; DOI: 10.1158/0008-5472.CAN-09-0994

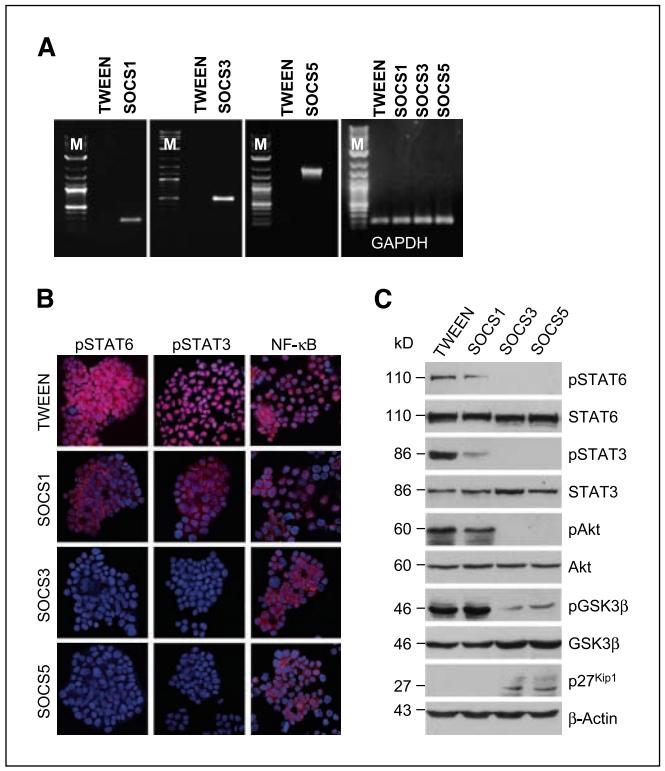

Figure 3. Exogenous expression of SOCS1, 3, and 5 affects STATs phosphorylation and PI3k/Akt activation. *A,* RT-PCR analysis in freshly isolated UTC cells infected with empty vector (TWEEN), SOCS1, SOCS3, or SOCS5 for SOCS1, SOCS3, or SOCS5 mRNA. Normalization was done by using GAPDH gene as housekeeping control. *B,* immunofluorescence analysis of UTC cytospun cells infected as in *A* stained for anti-pSTAT6, pSTAT3, and NF-κB (*red*). Nuclei were stained with Toto-3 iodide (*blue*). *C,* immunoblot analysis of pSTAT6, pSTAT3, pAkt, pGSK3β, and $p27^{Kip1}$, in UTC-infected cells as in (*A*). Detection of STAT6, STAT3, Akt, GSK3β, and β-actin as loading control. One representative of five immunoblots and one of three immunofluorescence analyses is shown.

committee. UTC cells (5×10^5) transduced with empty vector and SOCS3 were suspended in 200 μL of PBS and s.c. injected on both flanks of nude mice. After 7 d, when tumors were established, six mice per group were treated i.p. with Taxol, Doxorubicin, or 0.02% DMSO as control. Drugs were injected on days 1 and 3 of a 7-d cycle for four cycles at the concentration of 10 μmol/L in 200 μL for Taxol and 4 mg/Kg in 200 μL for Doxorubicin, of DMEM containing 0.02% DMSO. Tumor mass size was calculated weekly up to 4 wk according to the formula: $(\pi/6) \times$ larger diameter $\times$ (smaller diameter)^2.

Statistical analysis. Data of cell viability were analyzed by one-way unpaired ANOVA followed by a Student's *t* test to determine individual differences between TWEEN and SOCS1, TWEEN and SOCS3, TWEEN and SOCS5, and SOCS3 and SOCS5-infected UTC cells. *P* values of <0.05 were considered significant. Intensity of band signals in exposed film was determined by densitometric scanning and analyzed using NIH IMAGE software version 1.62 (by Wayne Rasband, NIH, Research Services Branch, NIMH). Results were expressed as protein/β-actin absorbance ratio.

Results

JAK/STAT and PI3K/Akt pathways are activated in thyroid cancer cells. To elucidate the mechanisms through which IL-4/IL-10 control resistance to cell death stimuli in thyroid cancer, we first investigated the activation of JAK/STAT and PI3K/Akt pathways in freshly purified thyroid cancer cells through the analysis of the phosphorylation levels of their target components. Immunoblot analysis revealed that phosphorylated JAK1 (pJAK1), STAT6 (pSTAT6), and STAT3 (pSTAT3) were highly expressed in all histologic subtypes of thyroid cancer examined (PTC, FTC, and UTC) compared with normal thyroid cells (Fig. 1*A*). Similarly, purified thyroid cancer cells showed increased levels of phosphorylated forms of Akt (pAkt) and glycogen synthase kinase-3β (pGSK3β) when compared with normal thyrocytes, both by immunoblot (Fig. 1*A*) and immunohistochemistry analysis (Fig. 1*B*).

Phosphorylation of GSK3β by Akt renders GSK3β inactive avoiding as a consequence cyclin D1 turnover (15). Akt regulates cell division also by inactivating $p27^{kip1}$ either by regulating its mRNA expression or by controlling its subcellular localization (16, 17). Accordingly, immunoblot analysis revealed increased expression levels of cyclin D1 in tumoral versus normal thyroid cells, whereas $p27^{Kip1}$ was down-regulated in all the histotypes of thyroid carcinoma (Fig. 1*C*).

We additionally found that the phosphorylated IKKα/β kinase and its target IκB-α were increased in thyroid cancer cells (Fig. 1*C*), and that NF-κB immunolocalized in the nuclei of purified PTC, FTC, and UTC cells (Fig. 1*D*), indicating that in thyroid cancer cells the activation of Akt cascade results in the enhancement of the NF-κB activity.

Thyroid cancer cells express low levels of SOCS family members. Because loss of expression of SOCS molecules has been reported in several human malignancies (18–22), we tested whether this could be the case of thyroid tumors, whose cytokine pathways were previously shown constitutively activated. For such purpose, purified epithelial cells from 10 PTC, 10 FTC, and 5 UTC, previously examined for positivity to IL-4 and IL-10 (data not shown), were analyzed by Real-Time PCR analysis for mRNA expression of SOCS1, SOCS3, and SOCS5, potent inhibitors of JAK/STAT activation. Similarly to control PBMCs, normal thyrocytes constitutively expressed the three SOCS molecules, which further increased in the presence of IL-4 and IL-10. In contrast, the expression of SOCS1, SOCS3, and SOCS5 was very low in thyroid cancer cells and not altered by cytokine exposure in the less differentiated hystotype (Fig. 2*A*).

Because of the three hystotypes analyzed, the anaplastic is the variant with the poorest prognosis, we aimed at testing whether exogenous expression of SOCS molecules could sensitize its cells to death both in *in vitro* and *in vivo.* Primary adherent cells are not tumorigenic in immunocompromised mice. Therefore, we purified thyroid cancer cells by depleting leucocytes and red cells from enzymatically dissociated UTCs and confirm their tumor-initiating capacity by s.c. injection in nude mice (Fig. 2*B*). Although UTC cells loose the tumorigenic potential after three *in vitro* passages, freshly isolated cells maintained a consistent tumorigenic activity in immunocompromised mice (Fig. 2*B*), confirming the possibility to obtain tumor xenografts without using classic cell lines. Moreover, immunofluorescence analysis revealed that IL-4, IL-10, and their respective receptors were present in freshly isolated thyroid cancer cells (Fig. 2*C*), in line with the hypothesis that the higher resistance to death of these cells could be due to IL-4/IL-10 activated pathways not counterbalanced by SOCS negative regulation.

SOCS1, SOCS3, and SOCS5 promote sensitization to chemotherapy through alteration of the Bcl-2 family members. To determine the ability of SOCS1, SOCS3, and SOCS5 to sensitize UTC cells to standard chemotherapy, we exogenously expressed SOCS genes by transducing freshly isolated UTC cells with lentiviral vectors carrying the GFP as reporter gene and SOCS1,

Published OnlineFirst July 28, 2009; DOI: 10.1158/0008-5472.CAN-09-0994

SOCS3, or SOCS5, or only GFP (TWEEN) as control. The efficiency of gene delivery was verified by monitoring GFP expression (data not shown) and by RT-PCR analysis for SOCS genes (Fig. 3*A*). We then confirmed the functional blockade of JAK/STAT signaling pathway in transduced cells by evaluating STAT6 and STAT3 phosphorylation levels. As shown in Fig. 3*B* and *C*, phosphorylation of STAT6 and STAT3 was reduced in SOCS1-infected cells and completely abolished by expression of SOCS3 or SOCS5. Similarly, phosphorylation levels of Akt and GSK3β were reduced in SOCS3 and SOCS5-infected cells, whereas $p27^{Kip1}$ was increased following their delivery (Fig. 3*C*). Moreover, NF-κB was found mainly in the cytoplasm of SOCS3 and SOCS5-infected cells, whereas localized both in the cytoplasm and in the nuclei of empty vector or SOCS1-infected cells (Fig. 3*B*). As a consequence, a significant reduction of UTC cell growth was observed (Fig. 4*A*), confirming the role of the JAK/STAT and PI3k/Akt pathways in thyroid cancer growth. To investigate the involvement of such pathway in UTC survival, cell viability of TWEEN, SOCS1, SOCS3, or SOCS5-infected cells exposed to Taxol or Doxorubicin for up to 72 hours was measured. We found that the expression of SOCS1, SOCS3, or SOCS5 sensitized UTC cells to chemotherapy-induced cell death (Fig. 4*B*). Although SOCS1-expressing UTC cells died moderately after exposure to drugs, SOCS3 expression was particularly effective in sensitizing UTC cells to chemotherapy, even more than SOCS5 after 24 and 72 hours of Taxol treatment or 24 hours of Doxorubicin treatment (Fig. 4*B*). Similar results were obtained by ethidium bromide staining (Fig. 4*C*). Altogether, these data indicate that JAK/STAT and PI3k/Akt pathways activation plays a major role in determining refractoriness of UTC cells to apoptotic stimuli because their blockade was able to restore the sensitivity to drug-induced death. To determine whether the increased sensitivity of UTC cells to chemotherapy promoted by SOCS proteins was related to the down-modulation of antiapoptotic molecules, we evaluated the expression of several proapoptotic and antiapoptotic proteins in UTC cells transduced with SOCS1, SOCS3, or SOCS5. We found alterations in Bak, Mcl-1, Noxa, Bcl-xL, Bcl-2, pBad, but not in Bax expression levels. In agreement with the survival data, SOCS3 and SOCS5 were able to produce the most significant alterations increasing the levels of Bak, Noxa, and the proapoptotic Mcl-1 short isoform (Mcl-1S), and reducing the expression of the antiapoptotic Mcl-1 long isoform (Mcl-1L) Bcl-xL, Bcl-2, and pBad, whereas SOCS1 seemed to exert little or no effect (Fig. 4*D*).

SOCS molecules control the expression levels of Bcl-xL through Akt down-modulation. To understand whether SOCS molecules control directly Bcl-2 family members' expression levels

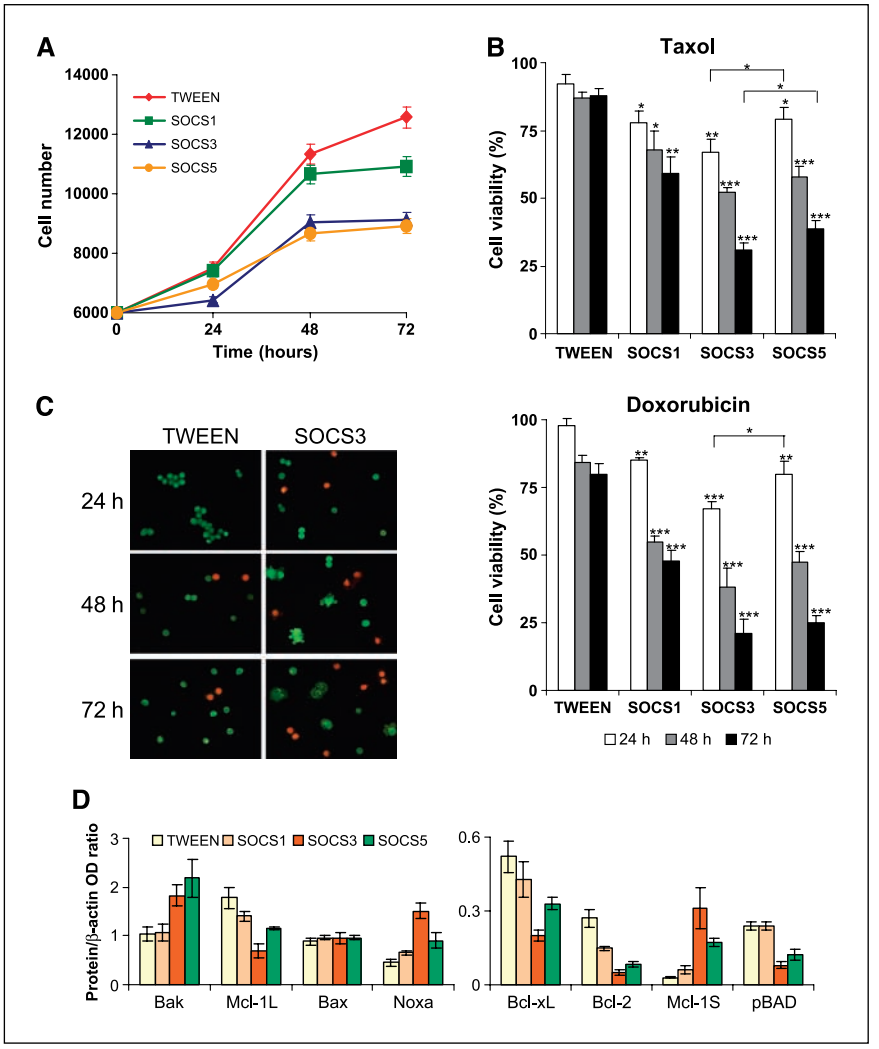

Figure 4. Exogenous expression of SOCS molecules sensitizes freshly isolated UTC cells to chemotherapy *in vitro* through alteration of the proapoptotic/antiapoptotic balance. *A,* cell growth of empty vector (TWEEN), SOCS1, SOCS3, or SOCS5-infected UTC cells up to 72 h. *B,* percentage of cell death in UTC cells infected as in *A* exposed to Taxol (5 μmol/L) or Doxorubicin (5 μmol/L) up to 72 h. *Columns,* mean of five independent experiment; *bars,* SD. *, $P < 0.05$; **, $P < 0.01$; ***, $P < 0.001$. *C,* representative ethidium bromide staining of UTC bulk cells infected with empty vector (TWEEN) or SOCS3 (*green,* viable cells; *red,* dead cells) following 24, 48, or 72 h of Doxorubicin treatment. *D,* relative band densities of Bak, Mcl-1L, Bax, Noxa, Bcl-xL, Bcl-2, Mcl-1S, and pBad in UTC bulk cells infected as in *A*. One representative of three independent experiments is shown.

Published OnlineFirst July 28, 2009; DOI: 10.1158/0008-5472.CAN-09-0994

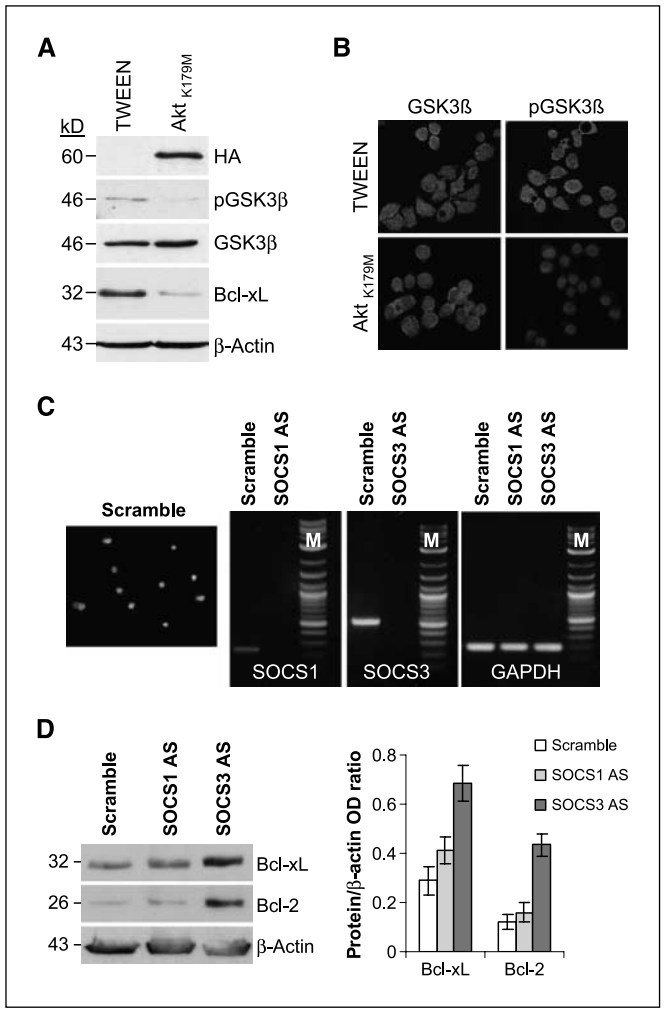

Figure 5. SOCS molecules control the expression levels of Bcl-2 family members through Akt down-modulation. *A,* Western blot analysis of HA, pGSK3β, and Bcl-xL in UTC cells infected with empty vector (TWEEN) or Akt_{K179M}. Loading control was performed by using GSK3 or β-actin. *B,* immunofluorescence analysis of GSK3β and pGSK3β (*red*) in UTC-infected cells as in *A*. Nuclei were stained with Toto-3 iodide (*blue*). *C,* fluorescent signal from normal thyrocytes transfected with scramble oligonucleotide (*left*) and RT-PCR analysis for SOCS1 and 3 in the same cells transfected with antisense oligonucleotides against SOCS1 or SOCS3 (*middle*). Normalization was done by using GAPDH gene as housekeeping control (*right*). *D,* immunoblot analysis of Bcl-xL and Bcl-2 in transfected cells as in *C* with their relative band densities. Detection of β-actin was used as loading control. One representative of three independent experiments is shown.

or indirectly through the Akt pathway, we expressed in UTC cells the HA-tagged Akt_{K179M}, a kinase-defective Akt mutant. The efficiency of gene delivery was verified by immunoblot analysis for HA (Fig. 5*A*). Moreover, we confirmed the functional blockade of Akt signaling pathway in Akt_{K179M}–transduced cells by evaluating GSK3β phosphorylation levels both by immunoblot and immunofluorescence analyses (Fig. 5*A* and *B*). Importantly, as revealed by immunoblot analysis, Bcl-xL was significantly reduced following inhibition of Akt kinase activity, indicating that in UTC cells the expression of Bcl-2 family members is regulated by Akt signaling pathway (Fig. 5*A*). Thus, the proapoptotic effect obtained following SOCS gene delivery is mediated by Akt. Moreover, we examined the effect of SOCS1 and 3 antisense oligonucleotide silencing on Bcl-xL and Bcl-2 expression in normal thyrocytes. Transfection efficiency was verified by monitoring fluorescent signals from thyrocytes transfected with scramble control oligonucleotide (scramble) and by RT-PCR for SOCS1 or SOCS3 in cells transfected with antisense RNA oligonucleotide directed to SOCS1 (SOCS1 AS) or SOCS3 (SOCS3 AS; Fig. 5*C*). Silencing of SOCS3 but not of SOCS1 resulted in increased Bcl-xL and Bcl-2 levels (Fig. 5*D*), confirming that SOCS3 controls the expression of both proteins in thyroid cells.

SOCS3 promotes *in vivo* sensitization to chemotherapy-induced cell death. Our *in vitro* data suggested that among the SOCS molecules analyzed, SOCS3 has major effect in restoring the sensitivity to chemotherapy-induced cell death in UTC cells. We therefore s.c. injected into nude mice UTC cells transduced with SOCS3-encoding or empty lentiviral vectors. After 7 days, mice were treated i.p. with Taxol, Doxorubicin, or DMSO as control. Interestingly, administration of Taxol or Doxorubicin to mice bearing tumors generated by SOCS3-transduced UTC cells dramatically reduced tumor growth up to 28 days (Fig. 6*A*). The extent of tumor growth inhibition obtained by Taxol or Doxorubicin treatment in xenografts generated by vector-transduced UTC cells was comparable with that induced by the sole expression of SOCS3 in the absence of the chemotherapic agent. Remarkably, Taxol or Doxorubicin treatment in the presence of SOCS3 expression resulted in a 3-fold decrease of tumor size compared with untreated control xenografts, and in a 2-fold decrease compared with either single chemotherapy or SOCS3 xenografts (Fig. 6*A*). Furthermore, H&E and A.M. stainings showed that residual tumors of the SOCS3-transduced UTC group treated with Taxol or Doxorubicin were largely fibrotic (Fig. 6*B*). TUNEL analysis confirmed that Taxol or Doxorubicin barely induced cell death in empty vector–transduced UTC cell–derived xenografts, whereas SOCS3 delivery enhanced the effect of chemotherapy leading to a significant increase of apoptotic events readily detectable in the few remaining cancer cells among the fibrotic areas (Fig. 6*B*). Moreover, phosphorylation of STAT6 and STAT3 was detected in the residual tumors of the empty vector–transduced UTC group but not in the group that has received SOCS3-transduced UTC cells (Fig. 6*B*). These results clearly indicate the promising effect of SOCS3 delivery in the treatment of UTC, suggesting that interfering simultaneously with IL-4 and IL-10 function could represent a novel way to reduce cell survival and refractoriness of UTC cells to conventional therapy.

Discussion

Resistance to apoptotic stimuli of cancer cells is the basis for the failure of conventional therapy in UTC patients and consequently for dismal prognosis (23). It is well established that IL-4 and IL-10 are cardinal regulators of cancer cells viability through activation of survival pathways involving cellular intermediates, i.e., Akt, which mediates its antiapoptotic effect through phosphorylation of multiple downstream targets involved in apoptosis regulation (24). In thyroid cancer cells, IL-4 and IL-10 trigger the phosphorylation of STAT6 and STAT3 following JAK1 activation, and Akt substrates include GSK-3β and IKK. The constitutive activation of such pathways and the related refractoriness to death is likely to depend on impaired expression of inhibitors of IL-4/IL-10 signaling, such as SOCS 1, 3, and 5. Exogenous expression of SOCS genes is able to reduce cell growth and sensitizes UTC cells to chemotherapeutic agents both *in vitro* and *in vivo* by influencing the balance of proapoptotic and antiapoptotic pathways. SOCS molecules

Published OnlineFirst July 28, 2009; DOI: 10.1158/0008-5472.CAN-09-0994

affect the expression of Bcl-2 family members by hindering Akt activation, as suggested by the reduction in Bcl-xL expression following forced expression of a kinase-defective Akt mutant. Likewise, SOCS3 targeting resulted in the increase of Bcl-xL and Bcl-2 levels in normal thyrocytes. Importantly, because $p27^{Kip1}$ is negatively regulated by activated Akt, we can speculate that its increase after SOCS3 or 5 overexpression depends also on Akt inhibition. This is in contradiction with previous suggestions according which $p27^{kip1}$ could be regulated by the E3 ubiquitin ligase system, and degraded after associating with the SOCS box. However, a direct correlation between SOCS2 and $p27^{Kip1}$ has also been described in breast carcinoma and suggests that the loss of control of S phase entry, possibly relates to SOCS2 loss (25).

It is not clear why the three SOCS genes displayed different ability in increasing death susceptibility. It is presumable that despite the shared structural similarities, they regulate cytokines signal transduction in different ways. We found that SOCS3 and 5 molecules simultaneously interfere with both JAK/STAT and PI3k/Akt prosurvival programs. Although it cannot be excluded that other not fully characterized members of the SOCS family could restore thyroid cancer cell sensitivity to chemotherapeutic drugs, it is likely that SOCS3 and 5 play a major role in the regulation of IL-4/IL-10 pathways in thyroid cells.

In the normal rat thyroid cell line FRTL-5, TSH has been reported to induce SOCS1 and 3 expression and to alter the phosphorylation state of STATs (26). Therefore, SOCS expression in normal thyrocytes not exposed to IL-4 and IL-10 may result from TSH receptor signaling. In normal cells, SOCS genes levels are rapidly up-regulated following cytokine stimulation and probably degraded once the stimuli has ceased. In contrast, a decreased TSHR expression has been observed in UTC cells and seems to be correlated to high proliferation (27). Therefore, in such tumor types, neither TSH nor cytokine stimulation could induce SOCS genes transcription.

A question emerging from these data is the way to induce SOCS molecules expression in thyroid cancer patients. Aberrant methylation of SOCS promoter genes has been reported in a variety of human cancers and strongly correlates with reduced expression (18–22). It is likely that this mechanism is responsible for the absence of SOCS in tumors that maintain the expression of the TSH receptor. Further studies could be aimed at better understanding the mechanism of SOCS genes silencing in thyroid cancer, thus promoting the development of combination therapies with demethylating drugs in the clinic. This might be useful also in other cancers where such prosurvival pathways are constitutively activated.

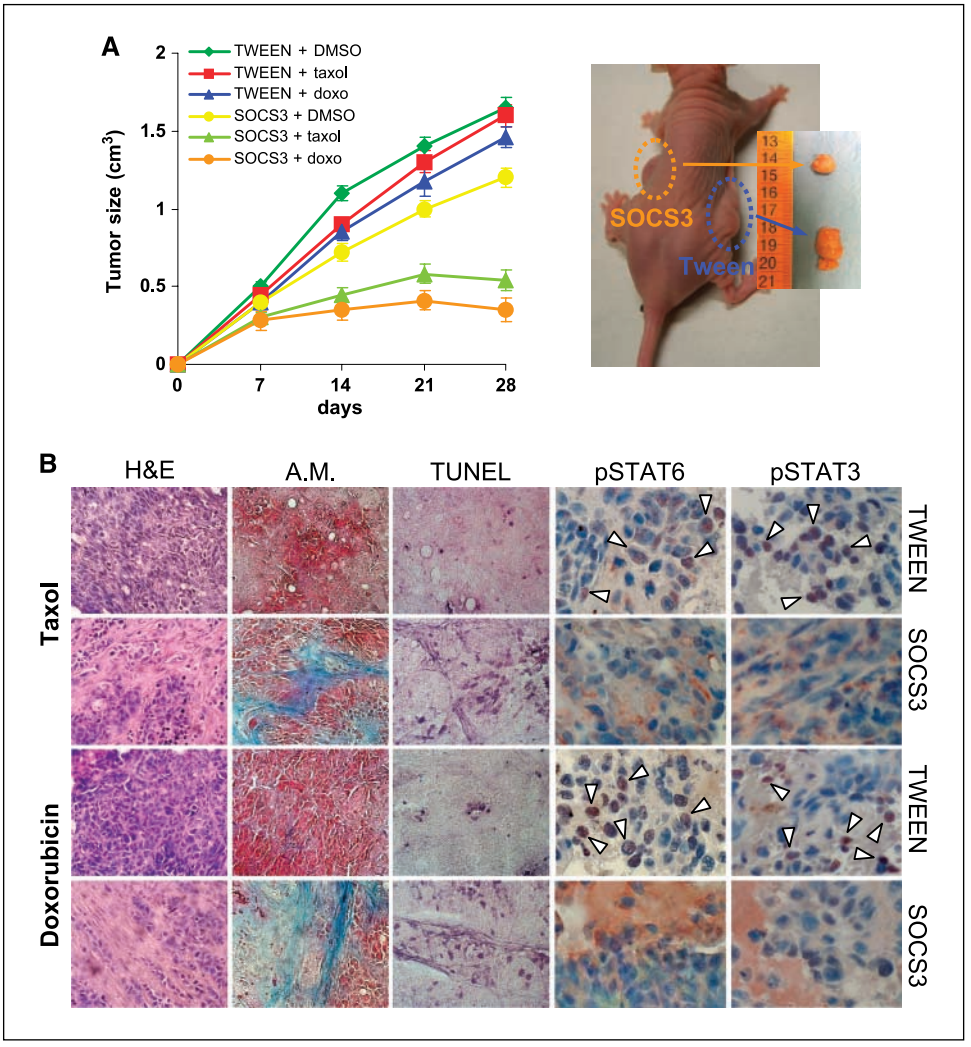

Figure 6. Exogenous expression of SOCS3 sensitizes UTC cells to chemotherapy-induced cell death *in vivo*. *A, in vivo* growth and size of s.c. xenografts derived from empty vector (TWEEN) or SOCS3-transduced freshly isolated UTC cells and i.p. treated with Taxol (5 μmol/L), Doxorubicin (4 mg/Kg), or DMSO. *Points,* mean of tumor size of six tumors per group; *bars,* SD. *B,* H&E, A.M., TUNEL (*nuclear dark blue color*), and pSTAT6/3 (*red color*) stainings on paraffin-embedded sections of tumors generated by UTC cells transduced with empty vector (TWEEN) or SOCS3 and treated with Taxol or Doxorubicin. Mice were sacrificed 24 h after the last cycle of chemotherapy treatment. *White arrowheads,* nuclear staining for pSTAT6 and pSTAT3. One representative of four independent experiments is shown.

Published OnlineFirst July 28, 2009; DOI: 10.1158/0008-5472.CAN-09-0994

Our results suggest that drug resistance in thyroid cancer cells is achieved by production of cytokines and loss of expression of tumor suppressor genes such as SOCS. We have already shown that IL-4 and IL-10 blockade restores the sensitivity to death in thyroid cancer cells (2, 3). Now, we provide evidence that exogenous expression of SOCS genes may represent another strategy to overcome UTC refractoriness to chemotherapy. This study identifies a second mechanism through which UTC cells escape from death stimuli, indicating a new possible therapeutic target for the most aggressive variant of thyroid carcinoma, which still remains associated with a very poor prognosis.

Disclosure of Potential Conflicts of Interest

No potential conflicts of interest were disclosed.

Acknowledgments

Received 3/16/09; revised 5/13/09; accepted 6/1/09; published OnlineFirst 7/28/09.

Grant support: Istituto Superiore di Sanità, Rome, Oncoproteomica, Italia-Usa prot. 527/B/3A/3 (G. Stassi). M.G. Francipane is a PhD student in Immunopharmacology at University of Palermo.

The costs of publication of this article were defrayed in part by the payment of page charges. This article must therefore be hereby marked *advertisement* in accordance with 18 U.S.C. Section 1734 solely to indicate this fact.

References

1. Schlumberger MJ. Papillary and follicular thyroid carcinoma. N Engl J Med 1998;338:297–306.
2. Stassi G, Todaro M, Zerilli M, et al. Thyroid cancer resistance to chemotherapeutic drugs via autocrine production of interleukin-4 and interleukin-10. Cancer Res 2003;63:6784–90.
3. Todaro M, Zerilli M, Ricci-Vitiani L, et al. Autocrine production of interleukin-4 and interleukin-10 is required for survival and growth of thyroid cancer cells. Cancer Res 2006;66:1491–9.
4. Todaro M, Lombardo Y, Francipane MG, et al. Apoptosis resistance in epithelial tumors is mediated by tumor-cell-derived interleukin-4. Cell Death Differ 2008;15:762–72.
5. Todaro M, Alea MP, Di Stefano AB, et al. Colon cancer stem cells dictate tumor growth and resist cell death by production of interleukin-4. Cell Stem Cell 2007;1:389–402.
6. Nelms K, Keegan AD, Zamorano J, Ryan JJ, Paul WE. The IL-4 receptor: signaling mechanisms and biologic functions. Annu Rev Immunol 1999;17:701–38.
7. Murray PJ. Understanding and exploiting the endogenous interleukin-10/STAT3-mediated anti-inflammatory response. Curr Opin Pharmacol 2006;6:379–86.
8. Rahimi AA, Gee K, Mishra S, Lim W, Kumar A. STAT-1 mediates the stimulatory effect of IL-10 on CD14 expression in human monocytic cells. J Immunol 2005;174:7823–32.
9. Hebenstreit D, Wirnsberger G, Horejs-Hoeck J, Duschl A. Signaling mechanisms, interaction partners, and target genes of STAT6. Cytokine Growth Factor Rev 2006;17:173–88.
10. Hebenstreit D, Luft P, Schmiedlechner A, Duschl A, Horejs-Hoeck J. SOCS-1 and SOCS-3 inhibit IL-4 and IL-13 induced activation of Eotaxin-3/CCL26 gene expression in HEK293 cells. Mol Immunol 2005;42:295–303.
11. Yoshimura A, Nishinakamura H, Matsumura Y, Hanada T. Negative regulation of cytokine signaling and immune responses by SOCS proteins. Arthritis Res Ther 2005;7:100–10.
12. Davey GM, Heath WR, Starr R. SOCS1: a potent and multifaceted regulator of cytokines and cell-mediated inflammation. Tissue Antigens 2006;67:1–9.
13. Ding Y, Chen D, Tarcsafalvi A, Su R, Qin L, Bromberg JS. Suppressor of cytokine signaling 1 inhibits IL-10-mediated immune responses. J Immunol 2003;170:1383–91.
14. Seki Y, Hayashi K, Matsumoto A, et al. Expression of the suppressor of cytokine signaling-5 (SOCS5) negatively regulates IL-4-dependent STAT6 activation and Th2 differentiation. Proc Natl Acad Sci U S A 2002;99:13003–8.
15. Diehl JA, Cheng M, Roussel MF, Sherr CJ. Glycogen synthase kinase-3β regulates cyclin D1 proteolysis and subcellular localization. Genes Dev 1998;12:3499–511.
16. Liang J, Zubovitz J, Petrocelli T, et al. PKB/Akt phosphorylates p27, impairs nuclear import of p27 and opposes p27-mediated G1 arrest. Nat Med 2002;8:1153–60.
17. Medema RH, Kops GJ, Bos JL, Burgering BM. AFX-like Forkhead transcription factors mediate cell-cycle regulation by Ras and PKB through p27kip1. Nature 2000;404:782–7.
18. Hatirnaz O, Ure U, Ar C, et al. The SOCS-1 gene methylation in chronic myeloid leukemia patients. Am J Hematol 2007;82:729–30.
19. He B, You L, Uematsu K, et al. SOCS-3 is frequently silenced by hypermethylation and suppresses cell growth in human lung cancer. Proc Natl Acad Sci U S A 2003;100:14133–8.
20. Komazaki T, Nagai H, Emi M, et al. Hypermethylation-associated inactivation of the SOCS-1 gene, a JAK/STAT inhibitor, in human pancreatic cancers. Jpn J Clin Oncol 2004;34:191–4.
21. Sutherland KD, Lindeman GJ, Choong DY, et al. Differential hypermethylation of SOCS genes in ovarian and breast carcinomas. Oncogene 2004;23:7726–33.
22. Tokita T, Maesawa C, Kimura T, et al. Methylation status of the SOCS3 gene in human malignant melanomas. Int J Oncol 2007;30:689–94.
23. Are C, Shaha AR. Anaplastic thyroid carcinoma: biology, pathogenesis, prognostic factors, and treatment approaches. Ann Surg Oncol 2006;13:453–64.
24. Nicholson KM, Anderson NG. The protein kinase B/Akt signalling pathway in human malignancy. Cell Signal 2002;14:381–95.
25. Farabegoli F, Ceccarelli C, Santini D, Taffurelli M. Suppressor of cytokine signalling 2 (SOCS-2) expression in breast carcinoma. J Clin Pathol 2005;58:1046–50.
26. Park ES, Kim H, Suh JM, et al. Thyrotropin induces SOCS-1 (suppressor of cytokine signaling-1) and SOCS-3 in FRTL-5 thyroid cells. Mol Endocrinol 2000;14:440–8.
27. Matsumoto H, Sakamoto A, Fujiwara M, et al. Decreased expression of the thyroid-stimulating hormone receptor in poorly-differentiated carcinoma of the thyroid. Oncol Rep 2008;19:1405–11.

Cancer Research
The Journal of Cancer Research (1916–1930) | The American Journal of Cancer (1931–1940)

AACR American Association for Cancer Research

Suppressor of Cytokine Signaling 3 Sensitizes Anaplastic Thyroid Cancer to Standard Chemotherapy

Maria Giovanna Francipane, Vincenzo Eterno, Valentina Spina, et al.

Cancer Res 2009;69:6141-6148. Published OnlineFirst July 28, 2009.